Research article

Muhammad Shaukat Khan*, Woheeb Muhammad Saeed, Bernhard Roth and Roland Lachmayer

Diffractive optics based automotive lighting system

A rear end lamp design for communication between road users

https://doi.org/10.1515/aot-2020-0055
Received September 21, 2020; accepted November 17, 2020; published online December 3, 2020

Abstract: Information projection using laser-based illumination systems in the automotive area is of keen interest to enhance communication between road users. Numerous work on laser-based front end projection employing refractive and reflective optics has been reported so far, while for rear end illumination efforts are more scarce and a different optical design concept due to limited volumetric size and field of view regulations is required. Here, we report on a new and versatile approach for a laser-based rear end lighting system for automotive application which enables projection of information or signals to support other road users. The design is based on thin diffractive optical elements projecting the desired patterns upon illumination. Also, for protection of the road users from the steering laser beam, a diffusive back projection screen is designed to project information while fulfilling both the field of view and safety requirements. The projection system is based on a periodic diffusive structure made of an array of biconic lenses with sizes in the millimeter range. The field of view (FOV) from the simulated lens arrays complies with the angular requirements set by the Economic Commission for Europe (ECE). As a proof of concept, the diffusive screen is fabricated using microfabrication technology and characterized. In future, the screen will be combined with thin diffractive optical elements to realize an entire integrated projection system.

***Corresponding author: Muhammad Shaukat Khan**, Hannover Centre for Optical Technologies, Leibniz Universitat Hannover, Nienburger Strasse 17, Hannover, 30167, Germany,
E-mail: muhammad.khan@hot.uni-hannover.de
Woheeb Muhammad Saeed and Bernhard Roth, Hannover Centre for Optical Technologies, Leibniz Universitat Hannover, Nienburger Strasse 17, Hannover, 30167, Germany
Roland Lachmayer, Inst. für Produktentwicklung und Gerätebau, Leibniz Universität Hannover, Welfengarten 1A, Hannover, 30161, Germany

Keywords: automotive lighting; diffractive optics; hot embossing; maskless lithography; microfabrication.

1 Introduction

Information projection for communication between road users is highly relevant in automotive [1–2]. This includes laser-based on-street projection as well as the lighting systems themselves which can be used for car-to-car and car-to-pedestrian communication. A variety of work has been done for front end projection so far [3–4]. For rear end illumination, light forming using refractive and reflective optical systems increases the volumetric size of the lighting system, often beyond acceptable limits. This can be mitigated by using thin diffractive optical elements (DOE) with coherent light sources, i.e. lasers, for light forming. Such DOEs exhibit typical structure sizes in the micro- and nanometer range, and flat surface relief DOEs can enable considerably smaller lighting components. Also, DOEs enable high diffraction efficiencies and can diffract incoming light at large diffraction angles. Multiple methods have been reported for fabrication of DOEs so far [5–8]. These methods strongly depend on the materials used, the speed of fabrication required and the cost. Fabrication of diffractive structures on glass substrates, for example, increases the cost and complexity of the process. On the other side, polymer materials such as polymethyl methacrylate (PMMA) provide an interesting alternative to glass, featuring both high optical transparency (>90%) and cost effectiveness. For fabrication of diffractive microstructures from polymer material various methods, i.e. laser direct wiring (LDW), mask-based photolithography and maskless photolithography have been reported [9–12]. The use of maskless photolithography systems enables faster and low-cost fabrication of microstructures on polymers. For this purpose, a spatial light modulator (SLM) is used to project the desired microstructure patterns into a photoresist material. The fabricated microstructure pattern upon illumination using laser light results in the desired output intensity distribution in form

of a projected signal or information. The initial microstructure pattern to be fabricated is computed using iterative algorithms as reported in [13], for example.

As for rear end laser-based lighting systems, the information is projected onto the outer lens of the optical system, which increases the laser exposure risk for other road users in case of failure. Hence, in a laser-based rear end lighting system, a nontransparent or partially transparent, i.e. a diffusive, outer lens is required. The function of this element is to diffuse the steering laser beam and display the desired pattern on its outer surface. Also, regulations set by the Economic Commission for Europe (ECE) for the field of view (FOV) must be considered [14]. In order to realize a diffuser with predefined FOV, different concepts based on grounded glass with irregular structures as well as engineered diffusers for beam shaping have been reported [15–16]. Also, the use of microlens array-based diffusers in LED streetlamps to increase uniformity and decrease glare effects have been achieved [17]. Furthermore, tandem microlens arrays producing top hat illumination patterns for epifluorescence microscopy and quantitative widefield imaging have been discussed [18]. Finally, randomly distributed microlens arrays have been employed for diffusing light beams at large angles and uniformities [19]. In this paper, we report on the design and the realization of a rear end automotive lamp system based on diffractive optics. The design of the DOE microstructure is based on binary gratings computed using a simple optimization algorithm. The fabrication of diffractive optical structures in polymer is achieved in a two-step process. The DOE microstructures are fabricated on photoresist using a self-developed maskless photolithography system and replicated onto polymer material using a lab-made hot embossing device. For proof of concept the required diffusive outer lens is designed and simulated in Zemax and manufactured using 3D printing.

2 System concept and regulations

The proposed lighting system consists of a coherent light source, i.e. laser diode, having a wavelength of 638 µm. The laser radiation illuminates the transparent polymer sheet with diffractive optical structures on its surface. The light from the DOEs is diffracted in the desired manner and projected on the diffusive outer lens, as shown in Figure 1. The latter then diffuses the intense diffracted laser beams at higher angles and ensures safety of other road users. Also, the diffuser projects the desired pattern in a required angular FOV set by the Economic Commission for Europe (ECE). As for the intensity of the light, it is dependent on the illumination source employed.

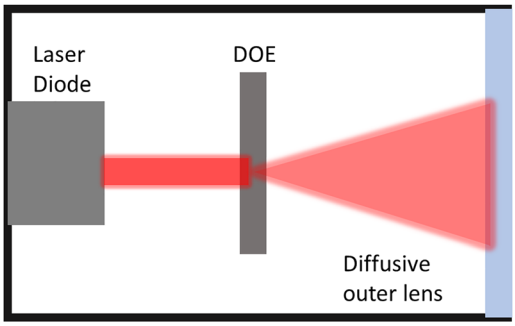

Figure 1: Concept of a laser based rear end automotive lighting system.

The standard intensity distribution of, for example, rear end S3 stop lamps defined in the ECE regulations is depicted in Figure 2(A). The standard light distribution displayed in Figure2(A) shows intensity distribution from −10° to +10° and −5° to +10° in horizontal and vertical direction, respectively. The FOV requirements for S1/S2 stop lamps is illustrated in Figure 2(B), comprising angles from −45° to +45° and −15° to +15° in horizontal and vertical direction, respectively. So, the light distribution of the newly developed system must be normalized to the horizontal and vertical intensity distribution requirements for S1/S2 stop lamps, as detailed below.

3 Fabrication of polymer-based diffractive microstructures

The diffractive polymer microstructures are fabricated in a two-step process. A maskless photolithography system is used for fabrication of the microstructure on photoresist and then a hot embossing system is used to replicate the fabricated structure on polymer, i.e. PMMA [20, 21]. The maskless photolithography system is based on a liquid crystal-on-silicon spatial light modulator (LCoS SLM), as illustrated in Figure 3(A). The SLM (Holoeye 6001) used has a resolution of 1080 × 1920 pixels, with each pixel having a size of 8 µm. A 450 µm LED is employed for illumination. The desired microstructure pattern is displayed onto the SLM screen using a built-in software provided with the SLM by *Holoeye Inc.*, see Figure 4(A). The diffractive microstructure profile pattern for a desired target illumination pattern is computed using iterative algorithms as described in [13]. Here, we give a brief description of the used algorithm only. The algorithm for calculating gratings period and orientation is based on a simple optimization problem. For a defined intensity distribution, depending on the number n of intensity spots in the desired distribution the

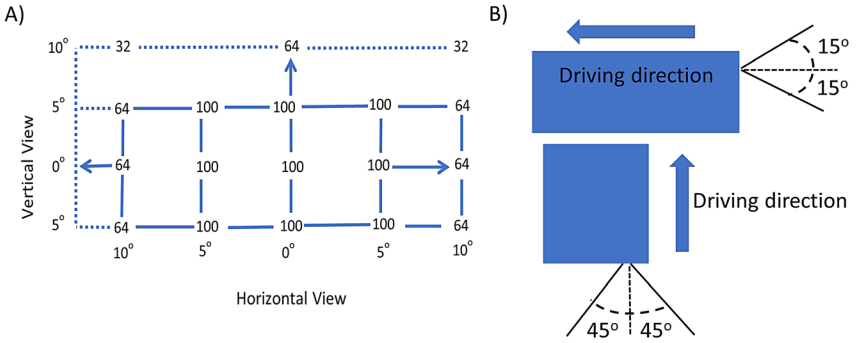

Figure 2: ECE regulations (A) Standard intensity distribution for S3 stop lamps, and (B) horizontal (top) and vertical (bottom) direction field of view requirements for S1/S2 stop lamps [14].

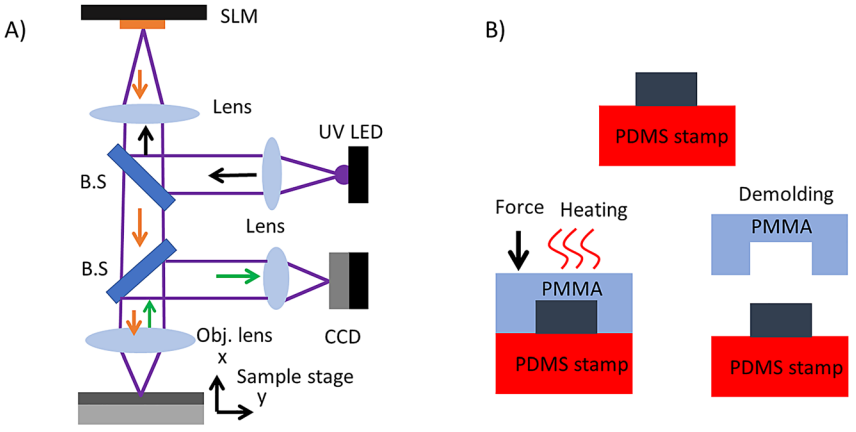

Figure 3: Fabrication of polymer microstructures. (A) Maskless photolithography process employing an SLM, (B) Hot embossing process.

required number of grating cells is determined. The algorithm starts with a $\sqrt{n}$ x $\sqrt{n}$ block of grating cells with each cell having a defined period Λ, and 0° orientation angle from the propagation axis. The far field distribution of the grating is obtained using:

$$I_G(x,y) = \frac{e^{ikz}e^{ik\frac{(x^2+y^2)}{2z}}}{j\lambda z} 2 - DFT\{G_{in}(\xi,\zeta)\}\Big|_{f_\xi=\frac{x}{\lambda z}, f_\zeta=\frac{y}{\lambda z}} \quad (1)$$

where, $G_{in}(\xi, \zeta)$ denotes the initial grating cell block, $I_G(x,y)$ the far field intensity distribution and $I_{Des}'(x,y)$ the desired intensity distribution. The far-field intensity of the grating cell block obtained using Eq. (1) consists of a line of intensity spots at the screen. The intensity distribution at the screen is mapped onto the desired intensity distribution. If the condition in Eq. (2) is satisfied, the (x,y) position for this grating cell is recorded, subsequently the grating period and the rotation angle as well. The orientation angle is increased till 180° if Eq. (2) does not hold:

$$(x,y) = \text{argmax}\{I_{Des}'(x,y) + I_G'(x,y) > I_{Des}'(x,y)\}; \quad (2)$$

The algorithm runs until, for n points in the desired intensity distribution, the corresponding (x, y) positions are obtained. From the positions the period and the orientation angle of all the grating cells is determined and the final microstructure profile pattern is computed and displayed onto the SLM screen for fabrication. The light from the SLM is projected onto the sample through an objective lens with a numerical aperture (NA) of 0.3 and a magnification of 10. The materials used are UV sensitive photoresists, i.e. (Shipley S1813 and Ormocomp) coated on silicon wafers using the spin coating technique. After exposure, the samples are developed using developers MF-26A and OrmoDev, followed by post exposure baking (PEB) steps.

The fabricated master wafer stamp containing binary phase gratings is then used to make an intermediate working stamp using PDMS (polydimethyl siloxane) casting which withstands high thermal loads. We used Elastosil® RT 607 A/B as a base and curing agent. The PDMS is poured onto the wafer stamp for curing at room temperature for 24 h. The working stamp is then used to replicate structures on polymethyl methacrylate (PMMA) foil having a thickness of 500 µm using the described in-house hot embossing system, as illustrated in Figure 3(B). The PDMS stamp is placed into the hot embossing system with PMMA foil on top. Another blank PDMS foil is placed on top of the PMMA foil to homogenize the force applied on the sample. The temperature of the system is increased to 140 °C, which

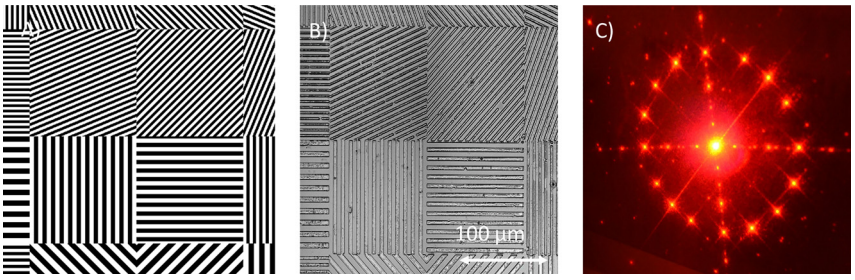

Figure 4: Diffractive microstructure. (A) Simulated diffractive structure profile, (B) fabricated and replicated diffractive structures on PMMA, and (C) desired intensity pattern upon illumination using laser light.

is above the glass transition temperature of PMMA ($T_g \approx 105$ °C). An embossing force of 7 kPa is applied onto the sample for 4 min. The sample is then cooled down to a demolding temperature of 60 °C and peeled off. The fabricated microstructures on PDMS stamp are replicated onto PMMA as shown in Figure 4(B).

The replicated binary microstructures are characterized by measuring the structure height and the period. A structure height of 338 and 322 µm is observed on the resist stamp and the PMMA replica, respectively, measured with confocal microscopy (Keyence, VHX-7000). A period of approx. 13.15 and 13.30 µm is found on the resist stamp and the PMMA replica, respectively. The difference in the replicated structure from the resist stamp is due to the thermal expansion of the PDMS during the embossing process. The structures on PMMA are illuminated with laser light at a wavelength of 632 µm and the resulting pattern can be seen in Figure 4(C). The measured diffraction efficiency from the fabricated binary grating in the first order is 44%. A higher diffraction efficiency can be achieved by fabrication of multilevel surface relief structures. A bright zero order diffraction or nondiffracted light can be seen in the middle of the pattern, see Figure 4(C). Similarly, higher diffraction orders can be seen with less intensity compared to the bright first diffraction order circular pattern. Each grating pattern with a defined orientation and period corresponds to a point in the image in Figure 4(C).

4 Diffusive outer lens system designs and realization

The next important component in the rear end light system is the diffusive outer lens, where the diffracted patterns are displayed. The lens design goal is to spread the light into a rectangular shaped profile as depicted in Figure 5 and described by the regulations mentioned in Section 2.

The diffracted beam from the diffractive optical element is projected onto the diffuser lens which spreads the light into a rectangular field of view, see Figure 5. For

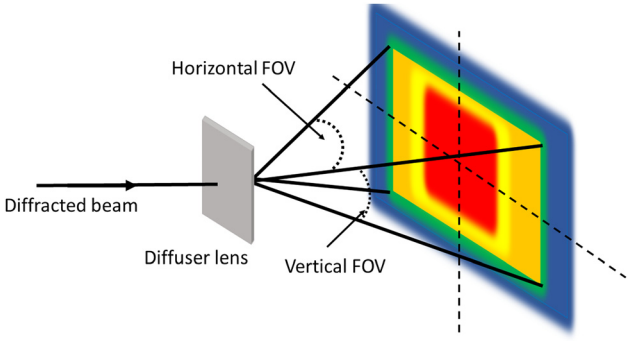

Figure 5: The design objective of the diffusive lens, showing a rectangular intensity profile for horizontal and vertical field of view FOV.

designing purposes, a diffuser surface with irregular structure profile and size leads to less freedom in design and optimization. In addition, the optimization procedure takes longer. Structures with regular structure profiles such as microlens arrays (MLAs) allow for variation in the output intensity distribution by changing lens shape parameters and usually require less optimization time. We have used Zemax Optics Studio software to simulate the diffuser shape for the desired FOV and the intensity profile. Multiple beam diverging lens profiles can be used such as biconcave or plano-concave lenses. For biconcave lens arrays the light beam can diffract at larger angles compared to the plano-concave lens design; however the computation time is increased due to multiple interfaces. On the other hand, plano-concave lens arrays require less computation time and form the light beam into a square shape profile. To achieve the rectangular intensity distribution, as shown in Figure 5, a biconic lens is selected where the conic constant and base radius of both the x and y axes can be varied and used as optimization parameters. Hence, the output intensity profile can be controlled in both horizontal and vertical directions. Also, a square geometry of the lens has been selected for a 100% fill factor. The outer side of the lens is kept flat, which means the conic constant of this interface is infinity, see in Figure 6(A). The sag equation defining the depth of the lens surface curve in

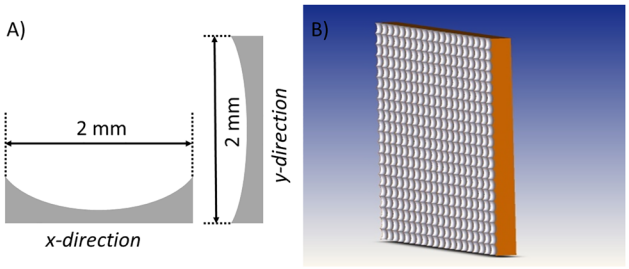

Figure 6: Biconic lens scheme. (A) Single lens side view with different radii of curvature in *x*- and *y*-directions, and (B) lenslet array composed of multiple single lenses.

the *x*- and *y*-directions for the biconic lens by the conic constant and the radius of curvature for a single lens is given by:

$$z = \frac{(c_x x^2 + c_y y^2)}{1 + \sqrt{1 - (1 + k_x)c_x x^2 + (1 + k_y)c_y y^2}}$$

$$c_x = \frac{1}{R_x} \tag{3}$$

$$c_y = \frac{1}{R_y}$$

where k_x and k_y are the unitless conic constants, R_x and R_y the radii of curvature in x and y direction, and c_x and c_y their reciprocal values, respectively. A flat top beam is required and simulated to ensure that the diffuser distributes the incoming laser light at a wavelength of 638 µm into a desired rectangular shape and desired intensity profile, see Figure 6, rather than expanding the Gaussian beam profile. The flat top beam is used to illuminate the diffusive screen to simulate the desired rectangular FOV, see Figure 7.

For the simulation of the diffuser lens, an array of lenses having an area of $12 \times 12\ \text{cm}^2$ is created. The material used for the lens also plays an important role with regards to transmission efficiency of the lenslet array. We have selected a glass material N-Lak 34 having a refractive index of 1.72 at a wavelength of 638 µm and a transmission efficiency of approx. 99.9%. The obtained radii of curvature of a single biconic lens in the lenslet array after the optimization are 1.05 and 4 mm and the conic constants –0.5 and 1 in *x* and *y* directions, respectively. The flat top beam is projected onto the diffuser and a rectangular FOV is observed on the detector placed at 24 cm from the diffuser surface, see Figure 8(a). Also, for the intensity profile obtained along the horizontal axis, the FOV ranges from –45° to +45° in close agreement to the normalized intensity distribution, see Figure 8(B). The intensity distribution of the S1/S2 lamp is derived from the standard light distribution of S3 lamps given in the ECE regulations (see Figure 2(A)).

As a proof-of-concept, due to unavailability of a glass processing system, we have fabricated the designed diffuser on PMMA using 3D printing. The printing of the diffuser part is done using an AGILISTA-3200W 3D printer system with the help from *Keyence Deutschland GmbH*. The thickness of the fabricated PMMA diffuser is 4 mm with each biconic lens measuring 2 mm. An image of a part of the fabricated diffuser as obtained using a confocal microscope (Keyence VHX-7000) can be seen in Figure 9(A). Also, the difference in the radius of curvature along the *x*- and *y*-axes can be noted in Figure 9(B and C). The measured pixel pitch or the centre-to-centre distance between two consecutive lenses is 2.2 mm. For measuring the intensity distribution from the fabricated diffuser, the diffuser is placed in front of the laser diode having a wavelength of 632 µm and upon illumination, the resulting intensity distribution shown in Figure 10(B) is obtained. The designed diffuser is characterized in terms of the transmission efficiency. This efficiency is obtained using the relation $\eta_t = P_t/P_i$, where η_t, P_t and P_i are the transmission efficiency, the transmitted power through the diffuser and the total input power, respectively. The total power from the laser source is 10 mW and the measured transmitted power is 7.47 mW obtained using a powermeter (*ThorLabs S121C*). A transmission efficiency of 74.7% is achieved with some power loss due to reflection from the

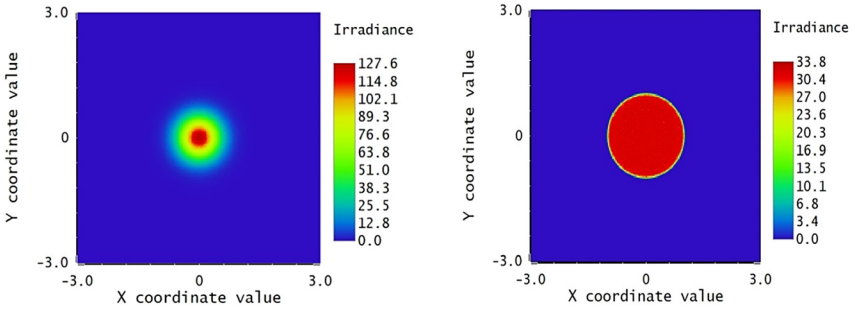

Figure 7: Flat top beam generation through the diffuser (right) achieved by a Gaussian beam used for illumination (left).

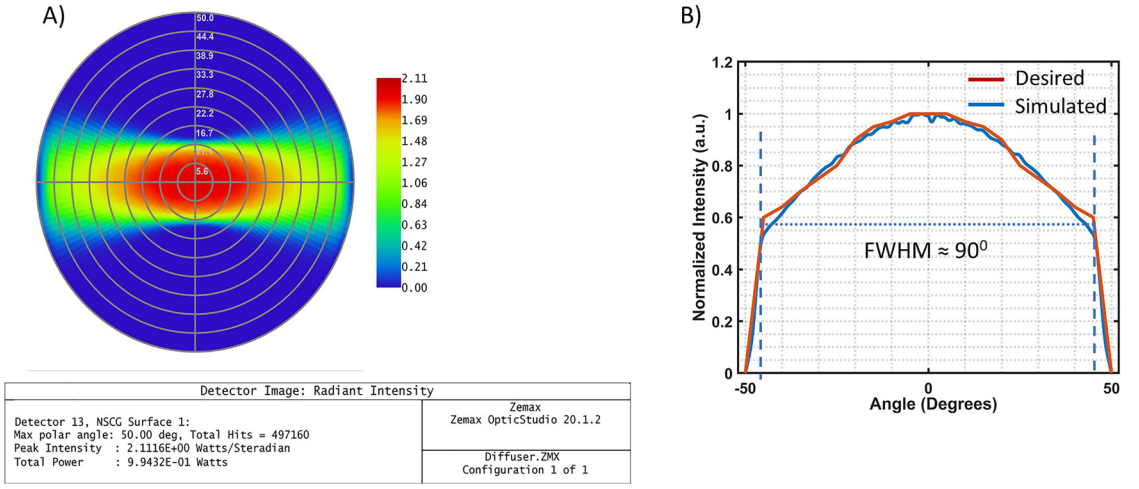

Figure 8: Simulation results from the diffuser. (A) The intensity distribution (FOV) at the detector placed at 24 cm from the diffuser surface, and (B) output intensity at the detector as a function of angle for the designed lenslet array diffuser.

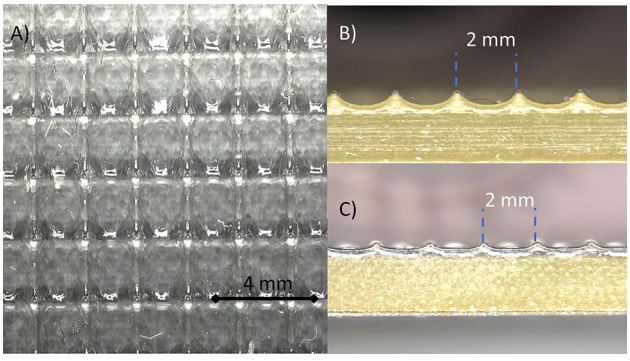

Figure 9: Fabricated diffuser on PMMA. (A) Microscopic image of the fabricated diffuser, (B) side view of the diffuser lens in *x*-direction, and (C) in *y*-direction.

diffuser surface. This loss is due to fabrication artifacts. The diffuser is designed with a flat top beam, and the required beam profile is realized by an appropriate design of the DOEs. As by design, the diffuser material is N-Lak 34 glass having a refractive index of 1.72, a difference in the final intensity distribution is observed in comparison the simulated distribution, see Figure 10(B). The change in the simulated FOV, as indicated in Figure 8(A), is due the change of the refractive index of the material and the finishing of the lens arrays.

For coherent illumination, speckle patterns usually appear due to interaction with rough surfaces or change in the refractive index of the propagating medium. Ultimately, these patterns originate from the interference of multiple wavefronts. As the diffuser in our work is illuminated with a laser beam, speckles are observed, see Figure 10(B). The reduction of the speckles can be achieved by modulation of the illumination laser beam or the optical element to change the coherence length of the individual wavefronts. This will be done in the next step in our work [22].

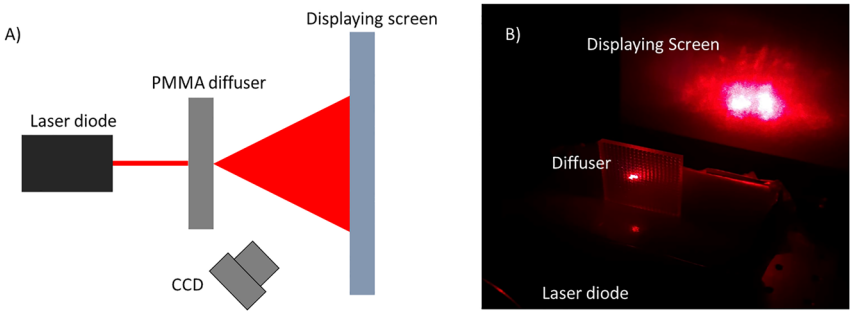

Figure 10: Schematic of (A) the measurement setup, and (B) image of the resulting intensity distribution from the diffuser upon illumination.

5 Conclusion

In this work, we have presented a new and versatile approach for a diffractive optics based rear end automotive lighting system. The approach is based on diffractive optical elements (DOEs) which diffract the incoming laser light in multiple diffraction orders forming a defined pattern. For a desired intensity distribution, the DOE profile structure can be fabricated with the developed maskless photolithographic system and a hot embossing device for replication on polymer. Upon illumination with a laser source the diffracted pattern from the DOE is projected onto the diffusive outer lens. The latter consists of a biconic lens array with a single lens area of 2×2 mm^2. The material chosen for the simulation of the lighting system is N-Lak 34 glass having a refractive index of 1.72 at a wavelength of 638 μm. For simulation in Zemax, the lens radius of curvature and conic constants are used as optimization parameter. The simulated lens array has a total area of 12×12 cm^2 and a thickness of 4 mm. The results obtained are in accordance with the ECE regulations in terms of geometrical visibility. The FOV simulated from the designed diffusive lens shows an angular visibility from −45° to +45° and from −15° to +15° with the reference point in horizontal and vertical direction, respectively. For proof-of-concept, we have fabricated the diffusive outer lens of 12×12 cm^2 using PMMA as material and 3D printing technology. The measured diffraction efficiency from the DOE and the transmission from the diffuser is 44 and 74.7%, respectively. The diffraction efficiency can further be increased by fabricating multilevel structures. Similarly, the transmission efficiency from the diffuser can also be increased by employing fabrication processes with good surface finishing of the diffuser and by reducing fabrication artifacts. The fabricated diffusive outer lens shows the desired rectangular intensity distribution upon illumination with laser light and ensures laser safety for other road users. In the next step, the thin DOE components and the diffusive outer lens will be combined, characterized, and optimized with respect to intensity and uniformity of the light distribution. In future, the entire system will be used to project signal functions to communicate with other road users.

Acknowledgement: We acknowledge the financial support provided by the Lower Saxony Ministry of Science and Culture (MWK) under PhD Program Tailored Light and the German Research Foundation DFG under Germany's Excellence Strategy within the Cluster of Excellence PhoenixD (EXC 2122, Project ID 390833453).

Author contributions: M.S. Khan, and B. Roth conceptualized the idea. M. Khan wrote the manuscript and carried out the experiments. M. Khan and W. M. Saeed did the simulations in Zemax. B. Roth and R. Lachmayer supervised the research. All authors proofread and improved the manuscript.

Research funding: Lower Saxony Ministry of Science and Culture (MWK) under PhD Program Tailored Light, and German Research Foundation DFG under Germany's Excellence Strategy within the Cluster of Excellence PhoenixD (EXC 2122, Project ID 390833453).

Conflict of interest statement: The authors declare no conflicts of interest regarding this article.

References

[1] A. Rasouli, K. Iuliia and J. K. Tsotsos, "Agreeing to cross: how drivers and pedestrians communicate," in *IEEE Intelligent Vehicles Symposium (IV)*, 2017, pp. 264–269.

[2] A. Habibovic, J. Andersson, V. M. Lundgren, M. Klingegård, C. Englund and S. Larsson, "External vehicle interfaces for communication with other road users?," in *Road Vehicle Automation*, vol. 5, Springer, 2019, pp. 91–102.

[3] P. P. Ley, M. Knöchelmann, G. Kloppenburg and R. Lachmayer, "Development methodology for optomechatronic systems using the example of a high-resolution projection module," *Proc. Des. Soc: Int. Conf. Eng. Design*, vol. 1, pp. 2547–2556, 2019.

[4] G. Kloppenburg, A. Wolf and R. Lachmayer, "High-resolution vehicle headlamps: technologies and scanning prototype," *Adv. Opt. Technol.*, vol. 5, no. 2, pp. 147–155, 2016.

[5] G. P. Behrmann and M. T. Duignan, "Excimer laser micromachining for rapid fabrication of diffractive optical elements," *Appl. Optic.*, vol. 36, no. 20, pp. 4666–4674, 1997.

[6] M.T. Gale, "Replication techniques for diffractive optical elements," *Microelectron. Eng.*, vol. 34, nos. 3-4, pp. 321–339, 1997.

[7] W. Däschner, P. Long, M. Larsson and S. H. Lee, "Fabrication of diffractive optical elements using a single optical exposure with a gray level mask," *J. Vac. Sci. Technol. B: Microelectronics and Nanometer Structures Processing, Measurement, and Phenomena*, vol. 13, no. 6, pp. 2729–2731, 1995.

[8] T. Hessler, M. Rossi, R. E. Kunz and M. T. Gale, "Analysis and optimization of fabrication of continuous-relief diffractive optical elements," *Appl. Optic.*, vol. 37, pp. 4069–4079, 1998.

[9] M. Rahlves, M. Rezem, K. Boroz, S. Schlangen, E. Reithmeier and B. Roth, "Flexible, fast, and low-cost production process for polymer based diffractive optics," *Optic Express*, vol. 23, no. 3, pp. 3614–3622, 2015.

[10] W. Watanabe, K. Matsuda, S. Hirono and H. Mochizuki, "Fabrication of diffractive optical elements in polymers by 400-μm femtosecond laser pulses," *J. Laser Micro Nanoeng.*, vol. 7, no. 1, p. 58, 2012.

[11] S. Schlangen, M. Ihme, M. Rahlves and B. Roth, "Autofocusing system for spatial light modulator-based maskless lithography," *Appl. Optic.*, vol. 55, no. 8, pp. 1863–1870, 2016.
[12] M. Rahlves, C. Kelb, M. Rezem, et al., "Digital mirror devices and liquid crystal displays in maskless lithography for fabrication of polymer-based holographic structures," *J. Nanolithogr. MEMS, MOEMS*, vol. 14, no. 4, 2015, Art no.041302.
[13] M. S. Khan, M. Rahlves, R. Lachmayer and B. Roth, "Polymer-based diffractive optical elements for rear end automotive applications: design and fabrication process," *Appl. Optic.*, vol. 57, pp. 9106–9113, 2018.
[14] European Commission for Economic, "Einheitliche Bedingungen für die Genehmigung von Fahrzeugen hinsichtlich des Anbaus der Beleuchtungs- und Lichtsignaleinrichtungen," *Regelung Nr*, vol. 48, 2016.
[15] R. Zhu, Q. Hong, Y. Gao, et al., "Tailoring the light distribution of liquid crystal display with freeform engineered diffuser," *Optic Express*, vol. 23, pp. 14070–14084, 2015.
[16] T. Guo, C. Yu, H. Li, C. Su, Y. Bian and X. Liu, "Microlens Array diffuser with randomly distributed structure parameters," *J. Phys. Conf.*, vol. 680, no. 1, 2016, Art no.012005.
[17] X. H. Lee, I. Moreno and C. C. Sun, "High-performance LED street lighting using microlens arrays," *Optic Express*, vol. 21, pp. 10612–10621, 2013.
[18] M. Jiri, M. Pospisilova, V. Svozil, et al., "Widefield imaging of upconverting nanoparticles on epifluorescence microscopes adapted for laser illumination with top-hat profile," *J. Biomed. Opt. 21*, vol. 5, 2016, Art no.056007.
[19] S. I. Chang, J. -B. Yoon, H. Kim, J. -J. Kim, B. -K. Lee, D. H. Shin, "Microlens array diffuser for a light-emitting diode backlight system," *Opt. Lett.*, vol. 31, no. 20, pp. 3016–3018, 2006.
[20] H. Becker and U. Heim, "Hot embossing as a method for the fabrication of polymer high aspect ratio structures," *Sensor. Actuator: Physical 83*, vol 1–3, pp. 130–135, 2000.
[21] N. Chiromawa and I. Kamarulazizi, "Effects of poly (methyl methacrylate) PMMA, film thickness in the light transmission through SiO2 for applications in solar cells technology," *Int. J. Eng. Innovative Technol.*, vol. 5, no. 1, pp. 125–131, 2015.
[22] M. Mohamed, M. A. Qianli, L. Flannigan and C. Q. Xu, "Laser speckle reduction utilized by lens vibration for laser projection applications," *Eng. Res. Expr.*, vol. 1, no. 1, 2019, Art no.015036.

Bionotes

Muhammad Shaukat Khan
Hannover Centre for Optical Technologies, Leibniz Universitat Hannover, Nienburger Strasse 17, Hannover, 30167, Germany
muhammad.khan@hot.uni-hannover.de

Muhammad Shaukat Khan received his Master's degree in Lasers and Photonics in 2016 from Ruhr Universität Bochum, Germany. Since 2016, he works at Hannover Centre for Optical Technologies in Hannover as a PhD student. His research topic focuses on diffractive optics in automotive lighting and sensing.

Woheeb Muhammad Saeed
Hannover Centre for Optical Technologies, Leibniz Universitat Hannover, Nienburger Strasse 17, Hannover, 30167, Germany

Woheeb Muhammad Saeed received his Master's degree in Optical Technologies from Leibniz Universität Hannover in 2020. Since 2019, he worked at the Hannover Centre for Optical Technologies in Hannover as a master student and completed his master thesis in 2020.

Bernhard Roth
Hannover Centre for Optical Technologies, Leibniz Universitat Hannover, Nienburger Strasse 17, Hannover, 30167, Germany

Bernhard Roth received the Ph.D. degree in atomic and particle physics from the University of Bielefeld, Bielefeld, Germany, in 2001, and the State Doctorate (Habilitation) degree in experimental quantum optics from the University of Duesseldorf, Duesseldorf, Germany, in 2007. From 2002 to 2007, he was a Research Group Leader with the University of Duesseldorf. Since 2012, he has been the Scientific and the Managing Director with the Hanover Centre for Optical Technologies and a Professor of physics with Leibniz University Hanover, Hanover, Germany, since 2014. His scientific activities include applied and fundamental research in laser development and spectroscopy, polymer optical sensing, micro- and nanooptics fabrication, and optical technology for illumination, information technology, and the life sciences.

Roland Lachmayer
Inst. für Produktentwicklung und Gerätebau, Leibniz Universität Hannover, Welfengarten 1A, Hannover, 30161, Germany

Roland Lachmayer studied Mechanical Engineering and received his diploma and PhD degrees from the Technical University Braunschweig in 1990 and 1996, respectively. He did research in the field of product development methodology. From 1996 to 2007, he worked as a development engineer, Head of department and Vice President for adaptive front lighting systems, research electronics and innovative project management with Hella KGaA, Hueck & Co. From 2007 to 2010, he was the Vice President in technical department by AEG Power Solutions AG. In 2010, he was appointed Full Professor and Head of the Institute of Product Development at the Department of Mechanical Engineering at Leibniz Universität Hannover (Germany). Since 2012, he is the Board Director of the Hanover Centre for Optical Technologies (HOT). Currently, Dr. Lachmayer teaches and researches in the field of optomechatronics, computer-aided engineering and development methodology. Dr. Lachmayer is a member of the 'Design Society', the German Branch of the European Optical Society (DGaO), and the German Society of Engineers (VDI).